Velocity distribution of Gold nanoparticles trapped on an optical waveguide

J. Patrick Hole and James S. Wilkinson

Optoelectronics Research Centre, University of Southampton, Highfield, Southampton, SO17 1BJ, United Kingdom

jph@orc.soton.ac.uk, jsw@orc.soton.ac.uk

http://www.orc.soton.ac.uk/ioms

Katarina Grujic and Olav Gaute Hellesø

Department of Physics, University of Tromsø, 9037 Tromsø, Norway

katarina@phys.uit.no, ogh@phys.uit.no

http://uit.no/fysikk/mikroelektronikk/9

Abstract: The velocity distributions of 250nm diameter gold nanospheres trapped in the evanescent fields of optical waveguides are studied. The automated analysis of a large number of particles and temporal frames is described. It is used to show that the envelope of the particles' speed follows the mode intensity profile of the evanescent field along a length of the waveguide and across its width. Modal beating in a dual-moded waveguide is mapped by analysis of nanoparticle distributions above the waveguide. A modal power of $\sim$150mW at λ=1066nm in a Cs^+ ion-exchanged monomode waveguide results in speeds of up to 500μm/s.

OCIS codes: (100.2960) Image analysis; (130.3120) Integrated optics devices; (140.7010) Trapping; (230.7380) Waveguides, channeled

References and links

1. K. Grujic, O.G. Hellesø, J.P. Hole and J.S. Wilkinson, "Sorting of polystyrene microspheres using a Y-branched optical waveguide," Opt. Express **13,** 1–7 (2005).
2. K. Grujic, O.G. Hellesø, J.S. Wilkinson and J.P. Hole, "Optical propulsion of microspheres along a channel waveguide produced by Cs^+ ion-exchange in glass," Opt. Commun. **239,** 227–235 (2004).
3. S. Kawata and T. Tani, "Optically driven Mie particles in an evanescent field along a channeled waveguide," Opt. Lett. **21,** 1768–1770 (1996).
4. L.N. Ng, M.N. Zervas, J.S. Wilkinson and B.J. Luff, "Manipulation of colloidal gold nanoparticles in the evanescent field of a channel waveguide," Appl. Phys. Lett. **76,** 1993–1995 (2000).
5. L.N. Ng, B.J. Luff, M.N. Zervas and J.S. Wilkinson, "Propulsion of gold nanoparticles on optical waveguides," Opt. Commun. **208,** 117–124 (2002).
6. T. Tanaka and S. Yamamoto, "Optically induced propulsion of small particles in an evenescent field of higher propagation mode in a multimode, channeled waveguide," Appl. Phys. Lett. **77,** 3131–3133 (2000).
7. T. Tanaka and S. Yamamoto, "Optically induced meandering Mie particles driven by the beat of coupled guided modes produced in a multimode waveguide," Japanese Journal of Applied Physics Part 2-Letters **41,** L260–L262 (2002).
8. A. Ashkin, J.M. Dziedzic, and T. Yamane, "Optical trapping and manipulation of single cells using infrared-laser beams," Nature (London) **330,** 769–771 (1987).

#6721 - $15.00 US
Received 11 March 2005; revised 11 May 2005; accepted 12 May 2005

9. M. Moskovits, "Surface-enhanced spectroscopy,". Rev. Mod. Phys. **57,** 783–826 (1985).
10. S. Kawata and T. Sugiura, "Movement of micrometer-sized particles in the evanescent field of a laser-beam," Opt. Lett. **17,** 772–774 (1992).
11. R.J. Oetama and J.Y. Walz, "Translation of colloidal particles next to a flat plate using evanescent waves," Colloids and Surfaces a-Physicochemical and Engineering Aspects **211,** 179–195 (2002).
12. P.B. Johnson and R.W. Christy, "Optical Constants of Noble Metals," Phys. Rev. B **6,** 4370–4379 (1972).
13. K. Svoboda and S.M. Block, "Optical trapping of metallic Rayleigh particles," Opt. Lett. **19,** 930–932 (1994).
14. H.J. Hagemann, W. Gudat, and C. Kunz, "Optical constants from the far infrared to the x-ray region: Mg, Al, Cu, Ag, Au, Bi, C, and Al_2O_3," DESY Rep. SR-74/7 Hamburg, Germany, (1974)
15. D.W. Lynch and W.R. Hunter, "Optical properties of metals and semiconductors," in Handbook of optical constants of solids, E.D. Palik, ed., (Academic Press, Orlando, 1985), pp. 275–367.

1. Introduction

The optical propulsion of gold or dielectric particles on an optical waveguide has been reported by several groups [1-7], with proposed applications in sorting of biological species [1, 7, 8] and in chemical sensing by surface enhanced Raman spectroscopy [9]. Kawata and Tani first demonstrated the propulsion of 0.5μm gold and 1μm platinum particles on waveguides [3]. More recently, Ng showed that 40nm gold particles could also be propelled and demonstrated the effects of polarization, waveguide width and modal power on the speed of particles [3, 4]. The trapping and propulsion of latex particles of diameter 1μm or above, where the effects of Brownian motion are much smaller, have also been studied on a waveguide [1-3, 6, 7] and above a prism [10, 11]. Gold particles, which have higher polarisability per unit volume than latex spheres, are easier to trap [12] and propel for a given size. However reports have so far been limited to observing the velocities and trajectories of single particles or a small number of particles, and velocities of only a few tens of microns per second have been observed, limiting the potential for high-throughput sorting. Practical exploitation of this technique requires further quantification of the velocity through study of the collective motion of large numbers of particles, and access to higher velocities.

In this paper we use the axial force resulting from absorption by and scattering from many 250nm gold nanoparticles over many minutes to demonstrate (i) that propelled particles have a speed distribution that is dependent on their 3-D position over the waveguide and, (ii) that the modal beat pattern on the surface of a dual-moded waveguide may be tracked. Frame-by-frame analysis of images from a CCD camera has been used to determine accurate instantaneous speeds, and recording durations of up to 10 minutes have been used to obtain large data samples, providing statistically reliable data on particle motion over waveguides.

2. Experimental procedures

Cesium ion-exchanged waveguides were fabricated in a soda-lime glass substrate (Menzel, $n_{1066nm} \approx 1.503$) by photolithographically defining straight channels of widths between 2.5 and 11μm in an aluminium film evaporated onto the surface of the substrate. The substrate was then placed in a $CsNO_3$ melt at 450^oC for 6.5 hours, the aluminium removed and the edges polished.

A reservoir with dimensions 15x10x0.2mm, formed in a moulded polydimethylsiloxane (PDMS) elastomer was placed on the surface of the waveguides. 250$\pm$20nm gold particles (Agar Scientific) were diluted in deionised water to 10^6 particles/ml and were pipetted into the reservoir. A cover-slip was placed on top to seal the cell. Laser light at 1066nm (IPG Photonics) was butt-coupled into an end-polished waveguide with a polarization-maintaining single mode fibre and the output power monitored.

The particles were imaged onto a cooled CCD camera (QImaging) using a microscope operated in dark-field mode at 20x magnification and images were recorded on a PC every 50ms.

#6721 - $15.00 US Received 11 March 2005; revised 11 May 2005; accepted 12 May 2005

The background, including scattering from surface defects and particles stuck to the surface, was subtracted from each frame by removing the 'average' frame. Particles were then identified by requiring several (typically between 2 and 5) adjacent pixels to record intensities significantly above the background noise. Sequential frames were then compared to identify where each individual particle travelled. Information about the position and the displacement from the last position for each particle is recorded and the results collated. While errors in correctly identifying the same particle in sequential frames cannot be totally removed, we estimate that less than 0.5% of particle displacements calculated are incorrect.

3. Results

The first image of a typical movie is shown in Fig. 1. It shows the motion of particles with a 50ms temporal resolution on a single-mode waveguide. The waveguide has nominal width 3μm with a measured e^{-2} intensity spotsize of approximately 5.0μm width x 2.4μm depth, and an effective index of 1.5042 ± 0.0005, measured using prism-coupling. It can be seen from this image that the particles are represented by just a few pixels; the average of these pixels is used to quantify the position. The two weak parallel lines show the edges of the waveguide, which was produced by ion-exchange through the 3μm wide channel. The movie may be run by clicking on the image.

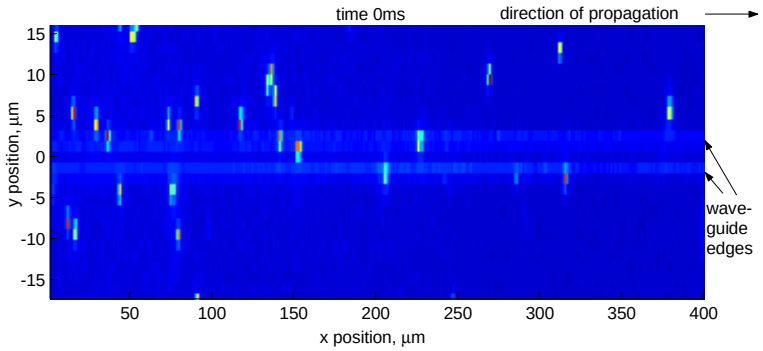

Fig. 1. Image showing particles above a 3μm wide, single-mode waveguide. The movie (1.8Mb) shows the motion of the particles - some of which are propelled along the waveguide.

Figure 2(a) shows the same small region within three consecutive images separated by 50ms, illustrating the motion of three particles on the same single-mode waveguide. While the images appear cluttered due to imperfections in the surface of the glass, this background is removed in the analysis; it is not removed here to allow the edges of the waveguide to be seen. It is clear that the particles do not move at a steady rate, for example the right particle (R) moves much further in the first 50ms than in the second 50ms, during which the left particle (L) shows no more than Brownian motion. This is believed to be due to fluctuations in the height and lateral position of particles above the waveguide resulting in them being exposed to differing evanescent field strengths.

Figure 2(b) shows the 2-D trajectory of an individual particle on the same waveguide for a duration of approximately 10s before it is propelled out of the field of view. It was extracted from a sequence of images containing many tens of particles. Alternating full and dotted lines connect the centre of the particle from sequential frames (every 100ms in this case). Brownian motion can be observed at the extreme left of the graph, as random meandering until the particle encounters the evanescent field of the waveguide. It is then propelled at a speed proportional

#6721 - $15.00 US
Received 11 March 2005; revised 11 May 2005; accepted 12 May 2005

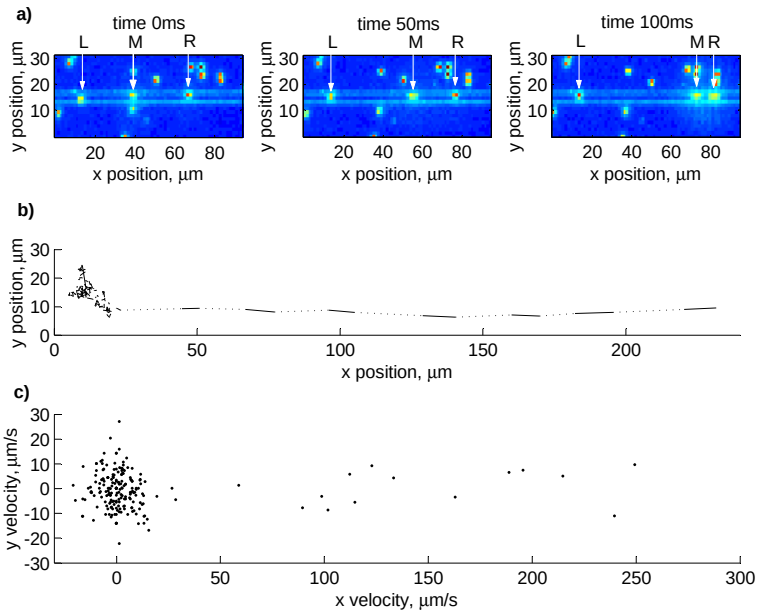

Fig. 2. a) Three consecutive images of three 250nm gold particles propelled along the waveguide b) A typical trace of a particle initially traveling randomly due to Brownian motion until it is propelled along the waveguide c) the velocity diagram of the particle in (b).

to the intensity at that point. The vector lines represent a velocity and can be represented as a distribution of velocities as shown in Fig. 2(c).

Figure 2(c) may be considered as two groups of points; the first is a near-circular distribution centered near the origin that represents random Brownian motion and any temperature-induced macro flow. The second group forms a lobe in the positive x direction. This represents the particle being propelled along the waveguide by the evanescent field of the mode. The transverse speed, compared with that under purely Brownian motion, is reduced slightly due to the restoring force from the lateral gradient of the optical trap.

Figure 3 shows the positions of all particles moving along the waveguide at a speed of at least 40μm/s, for (a) the monomode waveguide described in figs. 1 & 2 and (b) a laterally dual-moded waveguide, formed by ion-exchange on the same substrate through an 11μm wide stripe. For the dual-moded waveguide the input fibre is butted off-axis to excite both modes, which were measured (in air) to have effective indices of 1.5075 ± 0.0005 and 1.5090 ± 0.0005. These plots show that in the case of a single mode waveguide the particles follow a straight line along the waveguide, whereas in the case of the dual-moded waveguide the particles are only propelled in the areas following the beating pattern of intensity. The linear structure in these plots parallel to the waveguide is an artifact due to pixellation. In Fig. 2(b) the measured beat length is approximately 540μm, which would result from the beating between two modes with an effective index difference of $N_{eff} \sim 0.002$, in reasonable agreement with the measured effective indices. Particles travel on the high-intensity side of the waveguide until the intensity on both sides becomes similar, when they cannot cross over the waveguide as abruptly as the beat pattern does. Tanaka and Yamamoto demonstrated similar behaviour with 4μm diameter latex beads, but with much lower resolution due to the size of the beads [7].

Figure 4(a) & (b) shows the speed of particles along the waveguide as a function of their po-

#6721 - $15.00 US
Received 11 March 2005; revised 11 May 2005; accepted 12 May 2005

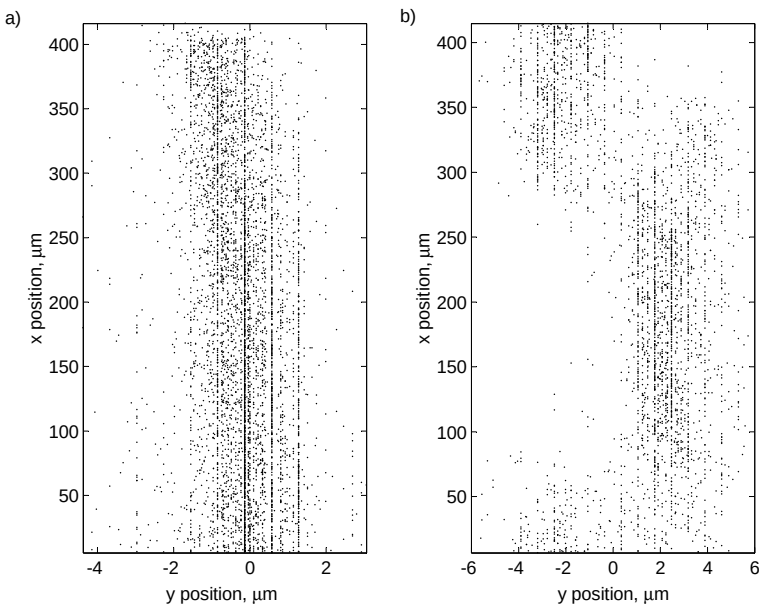

Fig. 3. Position of propelled particles for a) a single mode waveguide b) a dual-moded waveguide.

sition across the waveguide for both the single mode and dual-mode waveguides. These graphs represent a large number of particles observed over a waveguide length of $\sim 425\mu$m for approximately eight minutes. Figure 4(a) shows the case for the single mode waveguide while Fig. 4(b) shows the case for the dual-moded waveguide. Figure 4(a) clearly shows that at the centre of the waveguide, where the intensity is expected to be the greatest, the particles travel at the greatest speed. Figure 4(c) & (d) shows the measured mode profiles of the waveguides. The width of the distribution of the propelled particles for the single mode waveguide (4.4μm) shows that the propelled particles are confined within the 5.0μm width of the mode, as expected. In Fig. 4(d) only the fundamental mode is shown, to give an indication of the intensity distribution in comparison with the velocity distribution of the particles. In the experiment, both the fundamental and the first order mode are excited.

The envelopes of these data points represent the maximum velocity experienced by particles very close to the surface of the waveguide. The envelopes are "filled in" with data points at lower velocities as, at any instant, a particle may be at a different height above the waveguide, experiencing a weaker evanescent field and thus being propelled more slowly. The observed asymmetry is thought to be due to greater drift of particles from the right hand side onto the waveguide due to thermal effects. Figure 4(b) shows two maxima where the constructive interference of the modes gives a higher intensity than is obtainable at the centre of the waveguide.

In the case of the monomode waveguide, the maximum speed is approximately 500μm/s. In order to compare this to theory we equate the Rayleigh optical forces to the Stokes' drag forces to predict the velocity [4]. The peak intensity in the evanescent field of the waveguide was estimated to be $9GWm^{-2}$ per Watt of propagating modal power, using beam propagation analysis (RSoft), for which the refractive index distribution was taken from slab waveguides formed under the same conditions, and knowledge of the waveguide diffusion width. The model was confirmed by comparison with the measured effective index of the mode and the measured spot size. The modal power used (140mW) was estimated from the waveguide loss ($\sim$1dB/cm) and

#6721 - $15.00 US
Received 11 March 2005; revised 11 May 2005; accepted 12 May 2005

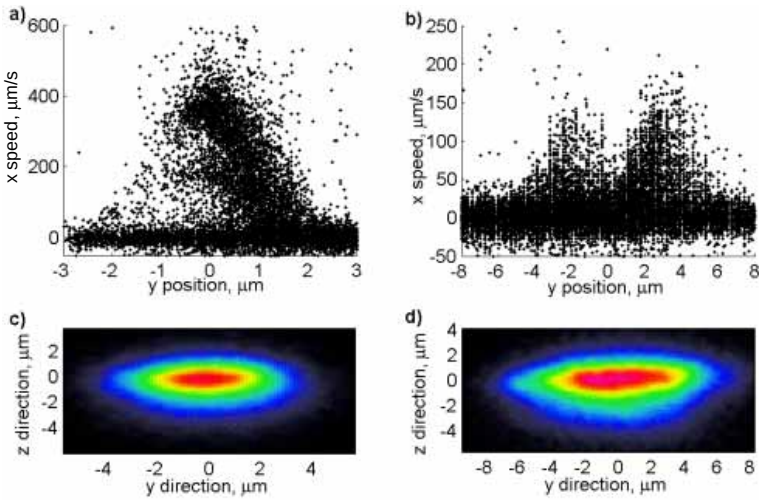

Fig. 4. Plot of lateral position against speed of particles for a) single mode waveguide b) dual-moded waveguide, and their respective beam profiles c),d).

the output power. This leads to a predicted velocity of 282μm/s. However due to the size tolerance of the particles, the predicted velocity for a 270nm particle is 385μm/s and 201μm/s for a 230nm particle emphasising the size sensitivity of the calculation. The gold permittivity, ε_g=-48.8+3.63i, is interpolated from data measured in [12]. This gives a penetration depth, δ_p, for the gold of 47nm at λ=1066nm, which is used in calculating the reduced volume for the polarisability due to the field's attenuation as described in [13]. It should be noted that the predicted velocity is strongly affected by the value of Im(ε_g), as the skin depth, δ_p, is inversely proportional to Im(ε_g) and as δ_p in turn strongly affects the polarisability of the particle. However Im(ε_g) has been reported as ranging from 3.6-5.9 for bulk gold [12, 14, 15] (and is not reported experimentally for particles in the relevant size range and wavelength). Here we use the lower value as it is the most often cited value. The agreement between theory and experiment (speeds up to 384μm/s predicted, with speeds of 500μm/s observed) is much improved on previous calculations [4].

4. Conclusions

In summary, the trapping and propulsion of large numbers of gold nanoparticles in the evanescent fields of optical waveguides has been described. The long recording times have allowed statistically significant quantification of the velocities of particles distributed in an evanescent field in the presence of Brownian motion. Automated processing has enabled identification and tracking of individual nanospheres within these populations. It has been found that particles do not travel at a constant speed, but that they have a broad distribution corresponding to the evanescent field intensity profile, that they will follow a modal beat pattern with nanospheres yielding high-resolution data, and that for optimised waveguides they are able to travel at speeds much higher than previously reported, with 500μm/s being achieved for a modal power of 140mW. These results show promise for the rapid manipulation of nanoparticles at surfaces, and provide detailed information on the temporal and spatial behaviour of collections of nanoparticles which will be essential for practical application.

#6721 - $15.00 US Received 11 March 2005; revised 11 May 2005; accepted 12 May 2005